

Spatial and temporal patterns of chronic wasting disease: fine-scale mapping of a wildlife epidemic in Wisconsin

ERIK E. OSNAS,^{1,5} DENNIS M. HEISEY,² ROBERT E. ROLLEY,³ AND MICHAEL D. SAMUEL⁴

¹Department of Forest and Wildlife Ecology, University of Wisconsin, 1630 Linden Drive, Madison, Wisconsin 53706 USA

²U.S. Geological Survey, National Wildlife Health Center, 6006 Schroeder Road, Madison, Wisconsin 53711 USA

³Bureau of Science Services, Wisconsin Department of Natural Resources, 2801 Progress Road, Madison, Wisconsin 53716 USA

⁴U.S. Geological Survey, Wisconsin Cooperative Wildlife Research Unit, 1630 Linden Drive, Madison, Wisconsin 53706 USA

Abstract. Emerging infectious diseases threaten wildlife populations and human health. Understanding the spatial distributions of these new diseases is important for disease management and policy makers; however, the data are complicated by heterogeneities across host classes, sampling variance, sampling biases, and the space–time epidemic process. Ignoring these issues can lead to false conclusions or obscure important patterns in the data, such as spatial variation in disease prevalence. Here, we applied hierarchical Bayesian disease mapping methods to account for risk factors and to estimate spatial and temporal patterns of infection by chronic wasting disease (CWD) in white-tailed deer (*Odocoileus virginianus*) of Wisconsin, USA. We found significant heterogeneities for infection due to age, sex, and spatial location. Infection probability increased with age for all young deer, increased with age faster for young males, and then declined for some older animals, as expected from disease-associated mortality and age-related changes in infection risk. We found that disease prevalence was clustered in a central location, as expected under a simple spatial epidemic process where disease prevalence should increase with time and expand spatially. However, we could not detect any consistent temporal or spatiotemporal trends in CWD prevalence. Estimates of the temporal trend indicated that prevalence may have decreased or increased with nearly equal posterior probability, and the model without temporal or spatiotemporal effects was nearly equivalent to models with these effects based on deviance information criteria. For maximum interpretability of the role of location as a disease risk factor, we used the technique of direct standardization for prevalence mapping, which we develop and describe. These mapping results allow disease management actions to be employed with reference to the estimated spatial distribution of the disease and to those host classes most at risk. Future wildlife epidemiology studies should employ hierarchical Bayesian methods to smooth estimated quantities across space and time, account for heterogeneities, and then report disease rates based on an appropriate standardization.

Key words: age prevalence; chronic wasting disease; CWD; direct standardization; disease mapping; emerging disease; epidemiology; hierarchical Bayesian model; *Odocoileus virginianus*; prion; space–time interaction; white-tailed deer.

INTRODUCTION

Describing the distribution and dynamics of infectious disease across a landscape is important for learning about and managing emerging diseases (Ostfeld et al. 2005, Lawson 2006) but is complicated by the space–time epidemic process, heterogeneities in the population of interest, sampling variance, and sampling biases. For example, heterogeneities that are often important are location, sex, or age because prevalence often increases with age and can differ between the sexes due to sex-specific behaviors or physiology that affect disease

exposure or susceptibility. These heterogeneities, in addition to sampling variance, may obscure observation of important disease trends that may be of interest to natural resource managers; therefore, sampling variance and non-spatial sample heterogeneities needed to be accounted for if meaningful representations of the spatial and temporal variation in disease patterns are to be examined.

Understanding the spatial distribution of a disease is often accomplished through applying statistical methods to data collected during disease surveillance and generating a map that describes spatial variation in risk. Disease mapping has a long history for human diseases (Bernardinelli et al. 1995, Waller et al. 1997, Elliott et al. 2000, Lawson 2006) but modern disease mapping methods have been applied to wildlife diseases less frequently (but see Farnsworth et al. 2006). The goal of mapping disease, at least implicitly, is to isolate and

Manuscript received 26 March 2008; revised 9 September 2008; accepted 28 October 2008. Corresponding Editor: N. T. Hobbs.

⁵ Present address: Department of Ecology and Evolutionary Biology, Princeton University, Princeton, New Jersey 08544 USA. E-mail: erik.osnas@gmail.com

display the role of location as a risk factor. When spatial samples are acquired, however, the spatial location is confounded with the age and sex structure of the sample. Therefore, observations of disease rates (incidence, prevalence, or force of infection) across a region can vary due to differences in age or sex structure of the sample in addition to any underlying location-specific variation. Traditionally, epidemiologists have recognized this problem and solved it by statistically estimating the effects of age, sex, or other heterogeneities and then standardizing rates to a common population before representing spatial variation (Ahmad et al. 2001, Szklo and Nieto 2007). While there are a variety of methods, direct standardization (a weighted average of rates across a population distribution of age, sex, or other strata) is very common (Ahmad et al. 2001) and has the advantage of expressing disease rates as an easily interpreted population average rather than as a strata-specific rate.

Disease rates are expected to show strong spatial and temporal dependence (autocorrelation) due to the epidemic process of local transmission and disease or host movement. The disease will initially be clustered near the point of introduction, then expand outward with time and increase at all locations to an endemic equilibrium, all of which may depend on local conditions (Keeling 1999, Smith et al. 2002, Hastings et al. 2005, Hosseini et al. 2006). Therefore, the spatial epidemic process creates heterogeneity in disease rates across space at any given time, and this pattern of heterogeneity across space may change with time as the epidemic progresses. The pattern of the spatial epidemic process is interesting because spatial and temporal changes in the disease distribution can be used to estimate the rate and direction of disease spread across a landscape (Moore 1999, Hosseini et al. 2006) or correlated with management actions (e.g., Conner et al. 2007).

As a risk factor, location is somewhat special relative to other risk factor covariates. One thing that distinguishes it from a typical covariate or regressor is that it is oriented and two-dimensional. In reality, location itself is essentially a proxy for unmeasured and missing covariates, which can include unmeasured spatial risk factors and the history of disease spread. In either case, this induces similarity between near-neighbors, resulting in an expected high degree of spatial dependence or autocorrelation. Spatial dependence is often treated as a nuisance to be removed before an analysis proceeds (Lichstein et al. 2002), however, spatial dependence can be used to reduce the influence of sampling variation by smoothing estimates across locations by “borrowing information” (Besag et al. 1991, Bernardinelli et al. 1995, Waller 1997, Best et al. 2005).

In this paper, we apply hierarchical Bayesian methods for disease mapping to understand the spatial and temporal distribution of chronic wasting disease (CWD) in Wisconsin. The hierarchical Bayesian methodology is

becoming widely used for complex statistical problems, especially in ecology and spatial epidemiology (Wakefield et al. 2000, Clark 2005, Clark and Gelfand 2006, Farnsworth et al. 2006, Lawson 2006, LaDeau et al. 2007), and the Bayesian methodology is especially valuable when estimates of disease rates (e.g., prevalence) at small scales are of interest; thus sampling noise is substantial. In addition, heterogeneity across host classes and spatial or temporal dependence may be important. Statistical models that include these effects are difficult or impossible to estimate with traditional methods (maximum likelihood or penalized quasi-likelihood). The hierarchical Bayesian methodology, however, is capable of estimating parameters of complex models with spatial dependence (Gelman et al. 2004, Best et al. 2005) and implementing such a model can smooth estimates to reduce sampling noise. We do not describe the full Bayesian methodology here, but refer the reader to Gelman et al. (2004) for a general treatment, and Farnsworth (2006), Clark (2005), Ellison (2004), and Wikle (2003) for ecological applications.

CWD is a neurological disease caused by an infectious prion affecting captive and free-ranging deer (family Cervidae) in North America. The disease was first recognized in captive deer in the 1960s and in free-ranging Colorado deer in 1981 (Williams et al. 2002). The distribution of the disease in North America is largely unknown because adequate surveillance has not been conducted in most areas of the continent (Samuel et al. 2003). CWD was first discovered in Wisconsin in 2002 from three deer that were shot in 2001 (Joly et al. 2003). After the discovery of CWD, the Wisconsin Department of Natural Resources (WDNR) initiated liberal deer hunting seasons and agency culling for disease surveillance and control (Blanchong et al. 2006, Joly et al. 2006).

CWD prion infection produces a lengthy asymptomatic period followed by inevitable mortality (Williams et al. 2002). Clinical signs develop at least 1.5 years after infection in captive mule deer and include changes in behavior, excessive salivation and water consumption, periods of somnolence, and loss of body condition (Fig. 1). In captive deer, the CWD prion can be transmitted by direct animal contact or indirectly from an environment contaminated with excreta or carcasses of infected deer (Williams et al. 2002, Miller and Williams 2003, Williams and Miller 2003, Miller et al. 2004, 2006). Infectious CWD prions have been found in body fluids of infected deer (Mathiason et al. 2006) and other prions bind to soils, which increases infectivity (Johnson et al. 2006, 2007).

We have three goals for this paper: (1) to describe the relationship between age, sex, and location on the probability of CWD infection in white-tailed deer (*Odocoileus virginianus*) across our study area, (2) to explore the spatiotemporal patterns for infection in this emerging epidemic, and (3) represent spatial variation in



FIG. 1. A CWD-infected 2.5-year-old white-tailed deer (*Odocoileus virginianus*) near Merrimac, Wisconsin, USA, on 9 October 2005. The deer was a regular visitor to Donald and Barbara Savoy's backyard for over a year. In the summer of 2005, the deer slowly lost weight and became progressively more disoriented over a six-month period (B. Savoy, *personal communication*). Finally, the deer began spending hours on the patio drinking out of bird baths (shown in photo), and Donald and Barbara realized that the deer might be infected; whereupon, the Wisconsin Department of Natural Resources gave permission to shoot the deer. On 11 October 2005 the deer was shot and subsequently tested positive by ELISA in the retropharyngeal lymph node and by IHC in the brainstem (obex). Photo credit: Donald Savoy, reproduced by permission.

prevalence by the method of direct standardization to a constant age and sex distribution across our study area.

METHODS

Data collection and study area

Deer were obtained by hunter harvest and limited culling by government sharpshooters across southern Wisconsin during five years: April 2002–April 2003 and fall hunting seasons (primarily September–January) from 2003 to 2007. For this paper, we applied the models described below to a 544-km² study area in southwestern Wisconsin (Fig. 2) because sampling and testing efforts were relatively constant across years and hunters were required to register every harvested deer. At registration, age, sex, and kill location to the quarter section (0.65 km²) were recorded for each deer. Deer ages (years) were determined by tooth replacement and wear (Severinghaus 1949) and classified by WDNR staff into eight categories (in years): 0.5 (fawn), 1.5 (yearling), 2.5, 3.5, 4.5–5.5, 6.5–8.5, 9.5–11.5, and ≥ 12.5 . For the present analysis, we only used deer collected from June 2002 to 30 April 2007. All deer collected in May of any year were deleted from the data set because it was unclear how to interpret the age code around the time of birth. For polynomial models of age deer age was then converted to a continuous variable by assuming that all

deer were born on 15 May, assigning the midpoint of the age interval to age classes that spanned multiple years, and summing the amount of time in years between 15 May of the birth year and the date of death. For all deer in this analysis, harvest year was assigned when the hunting season began (e.g., a deer killed between 1 June 2005 and 30 April 2006 would be assigned the harvest year 2005).

At registration, heads were removed from most deer >1 year old and a smaller fraction of fawns. Heads were transported to a tissue extraction center where a portion of the brainstem (obex) and retropharyngeal lymph nodes (RLN) were collected for CWD diagnosis at the Wisconsin Veterinary Diagnostic Laboratory, as described in Keane et al. (2008). All deer that tested positive in the RLN were considered positive for CWD.

Hierarchical Bayesian model for infection probability

The model used to estimate the probability of infection has three parts: (1) a data model that defines the likelihood, (2) a process model that defines the expectation of the data as a function the covariates, and (3) a set of prior distributions for the parameters. Finally, the output of the model is a posterior distribution for the parameters and/or functions of parameters.

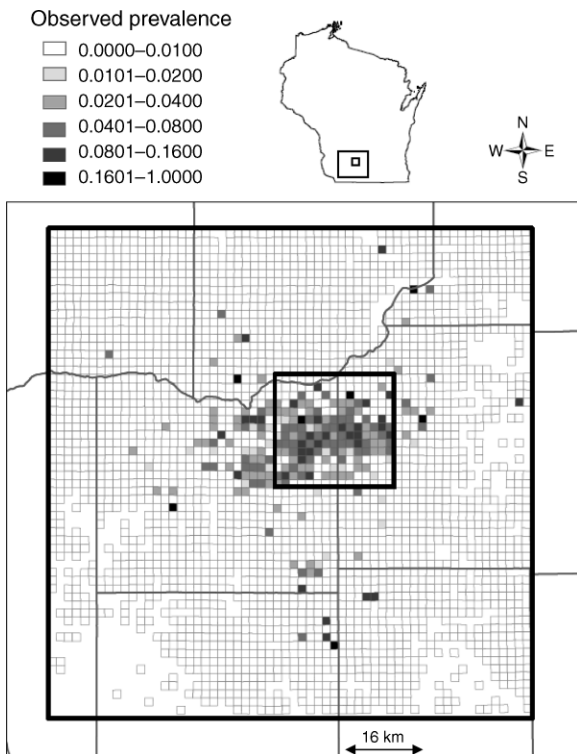


FIG. 2. Observed prevalence of deer samples from southwestern Wisconsin 2002–2007. Observed prevalence is the number of CWD-positive deer divided by the total deer tested for CWD in the local area (small grid cells). The small grid cells are sections (2.59 km²). Sections without a grid indicate that no deer were sampled. All analysis was restricted to a 544-km² study area (the small rectangle centered on the cluster of disease) because sampling effort in that area was relatively uniform across years and most positives were found in that area.

Data model.—Our data were the infection status for individual deer j in location i , Y_{ij} . We assumed that Y_{ij} was Bernoulli distributed with parameter p_{ij} , the probability of infection. As is typical, we assume that animals are independent conditional on their covariate profiles, which includes location, age, and sex.

Process models.—We fit two different sets of models. The first set was used to describe the location-, age-, sex-specific patterns in prevalence. The second set was used to describe temporal and spatiotemporal patterns, after accounting for the effects of location, age, and sex on p_{ij} . For all models, we used the complimentary log-log link function to describe how the probability of infection changed with individual-level covariates:

$$p_{ij} = 1 - \exp[-a_{ij}\exp(\mu_{ij})] \quad (1)$$

where p_{ij} is the probability of infection for an individual deer j at spatial location i , a_{ij} is the age of animal j , and μ_{ij} is the value of the covariate function for deer j at location i . Eq. 1 is often shown as the more familiar form of the complimentary log-log link function with age (a_{ij}) as an offset: $\log(-\log(1 - p_{ij})) = \log(a_{ij}) + \mu_{ij}$. Eq. 1 can be derived from a simple differential equation

describing an epidemic; where $a_{ij} \exp(\mu_{ij})$ estimates the cumulative infection hazard under the assumption of epidemic equilibrium and age-constant infection hazard (Grenfell and Anderson 1985, Caley and Hone 2002, Heisey et al. 2006). Thus, Eq. 1 is based on an underlying epidemiological process. It is important to note that $\exp(\mu_{ij})$ is multiplicative with an individual's age a_{ij} . Thus, for any age constant μ_{ij} there will be an increasing age-infection relationship after birth.

Eq. 1 was combined with the standard linear predictor in order to examine the effects of location, age, and sex on p_{ij} :

$$\mu_{ij} = \beta_0 + \mathbf{x}_{ij}\boldsymbol{\beta} + \alpha_i.$$

In this equation, β_0 is an intercept, \mathbf{x}_{ij} is a row vector of covariate values for each individual animal j at location i , $\boldsymbol{\beta}$ is the column vector of regression effects, and α_i is a latent spatial effect associated with location i . We fit various polynomial models of age and sex covariates (Table 1) to find the best parametric predictor for p_{ij} (Set 1, Models 1.1–1.5, Table 1). We coded the sex effect to equal one for males and zero for females. As an alternative to the parametric form of μ_{ij} , we next used $\mu_{ij} = \beta_0 + \beta_j + \alpha_i$ as the linear predictor (Model 1.6, Table 1), where j indexes each of the 16 age–sex categories. For this model, ages (a_{ij} , Eq. 1) were based on the tooth wear categories and we assigned the midpoint for age classes that spanned multiple ages. We then assumed that the effects β_j came from a Normal(0, τ^2) distribution, and we gave a prior distribution for τ^2 . This model also allowed us to explicitly test for changes in p_{ij} between age categories.

The second model set (2.1–2.4, Table 1) was used to explore the temporal and spatiotemporal effects after accounting for the effects of location, age, and sex. Here, we used the best age–sex model from Set 1 (Table 1) as a starting point and then added time and space-time effects to μ_{ij} . We first added a linear year effect to μ_{ij} (Model 2.1, Table 1). Year was coded such that the intercept (β_0) was the year 2002; therefore, the regression parameter estimated the spatially uniform year effect on μ_{ij} . Next, we fit a model where there was a unique random effect for each year β_k and a spatial effect common across years (Model 2.2, Table 1). We assigned a distribution to $\beta_k \sim \text{Normal}(0, \tau^2)$, and gave a prior distribution for τ^2 . This model relaxes the assumption of a linear effect with time but maintains the spatial homogeneity of the year effect. We allowed for spatial heterogeneity in the year effect on μ_{ij} by adding a spatial component to a linear year effect (Model 2.3, Table 1; Bernardinelli et al. 1995). Therefore, spatial dependence of the linear predictor was modeled as $\alpha_i = \gamma_i \text{year} + \delta_i$, where δ_i is spatial intercept effect for 2002 and γ_i is a spatially specific slope for year in μ_{ij} . Spatially specific slopes might be expected due to local variation in deer density, density of prion in the environment, the space-time epidemic process itself, or other location-specific factors. We next fit a model with unique intercepts and spatial effects for each location and year (Model 2.4,

TABLE 1. Structure of the linear predictor (μ_{ij}) for two different model sets for white-tailed deer (*Odocoileus virginianus*).

Model	Linear predictor (μ_{ij})
Set 1	
1.1	$\beta_0 + \beta_1 \text{sex}_{ij} + \alpha_i$
1.2	$\beta_0 + \beta_1 \text{sex}_{ij} + \beta_2 \text{age}_{ij} + \alpha_i$
1.3	$\beta_0 + \beta_1 \text{sex}_{ij} + \beta_2 \text{age}_{ij} + \beta_3 \text{sex}_{ij} \text{age}_{ij} + \alpha_i$
1.4	$\beta_0 + \beta_1 \text{sex}_{ij} + \beta_2 \text{age}_{ij} + \beta_3 \text{sex}_{ij} \text{age}_{ij} + \beta_4 \text{age}_{ij}^2 + \alpha_i$
1.5	$\beta_0 + \beta_1 \text{sex}_{ij} + \beta_2 \text{age}_{ij} + \beta_3 \text{sex}_{ij} \text{age}_{ij} + \beta_4 \text{age}_{ij}^2 + \beta_5 \text{age}_{ij}^2 \text{sex}_{ij} + \alpha_i$
1.6	$\beta_0 + \beta_j + \alpha_i$
Set 2	
2.1	Model 1.5 + $\beta_6 \text{year} + \alpha_i$
2.2	Model 1.5 + $\beta_k + \alpha_i$
2.3	Model 1.5 + $\beta_6 \text{year} + \gamma_i \text{year} + \delta_i$
2.4	Model 1.5 + $\beta_k + \varepsilon_{ik}$

Notes: For all models, i indexes spatial location and k indexes year. Model Set 1 describes the age, sex, and spatial random effects (α_i). In Models 1.1–1.5, j indexes covariates values of individual deer; in Model 1.6, β_j is a separate effect for each of 16 categories of tooth wear and sex indexed by j . Model Set 2 uses the best age–sex structure selected from Model Set 1, according to the DIC, and adds temporal and spatial–temporal effects. Set 2 includes a model (2.1) with a linear trend across years that is common across all locations (β_6) and spatial effects constant across years (α_i), a model (2.2) with categorical (random) effect across years (β_k), and a model (2.3) with a trend across years common to all locations (β_6) and a spatially variable intercept (δ_i) and trend across years (γ_i). Finally, set 2 contains a model (2.4) that includes a unique spatial effect for each year (ε_{ik}).

Table 1) after Waller et al. (1997). In this model, the year-specific intercept is β_k and the spatial effects are ε_{ik} ; k indexes year and i indexes the spatial location. This model is most flexible and allows for different spatial relationships for each year but has a large number of parameters. Code for select models is given in the Supplement.

Prior distributions.—We chose Normal prior distributions for all regression effects β in Set 1 and β_6 in Model 2.1 (Table 1). These priors had a mean of zero and a variance of 10. Extensive experimentation with other normal priors more or less informative determined that these were very noninformative. We gave β_0 , β_6 , and β_k improper flat prior distributions on the whole real line, as is necessary to implement the spatial random effects in our software (Spiegelhalter et al. 2004). The parameters τ^2 in Models 1.6 and 2.2 were given Gamma(0.5, 0.5) priors for the precision $1/\tau^2$.

All spatial effects (α_i , γ_i , δ_i , and ε_{ik}) were modeled as an “improper” intrinsic Gaussian conditional autoregressive (CAR) effect (Besag et al. 1991, Bernardinelli et al. 1995, Waller et al. 1997, Wakefield et al. 2000). The CAR random effect causes neighboring locations to have similar estimates and is widely used in disease mapping to implement spatial dependence (Lawson et al. 2003, Richardson et al. 2004, Best et al. 2005, Farnsworth et al. 2006). For any particular area i , the CAR effect has a normal distribution with a mean of the average of its neighbors and a variance that is inversely proportional to the number of neighbors:

$$\alpha_i | \alpha_{i+} \sim \text{Normal} \left(\frac{\sum_{(j \text{ in } i+)} \alpha_j / n_{i+}, \sigma^2 / n_{i+}} \right)$$

where $i+$ is the set of neighbors for area i , n_{i+} is the number of neighbors for area i , and σ^2 is the prior variance for α_i that is common to all areas. We used the four primary and four secondary areas as neighbors and gave them equal weights. The value of the variance parameter σ^2 controls the strength of spatial dependence. Zero variance implies complete spatial dependence and positive values indicate decreasing spatial dependence. The variance parameter σ^2 is given its own prior distribution (a “hyperprior”). We used a Uniform(0, 100) distribution for the hyperprior standard deviation, and experimented with Gamma(0.5, 0.5), Gamma(0.1, 0.1), and Gamma(0.5, 0.005) hyperpriors for the precision ($1/\sigma^2$) but could detect no difference in results. An additional constraint placed on the “improper” CAR model in our implementation software is that the α_i ’s sum to zero across the entire study area (Spiegelhalter et al. 2004).

Posterior distributions.—Posterior distributions were estimated using Markov chain Monte Carlo simulation implemented in the program WinBUGS (Lunn et al. 2000; Supplement). All quantities were estimated by samples from four Markov chains after they reached convergence. We initialized the four chains with different points in parameter space, and allowed a burn in period of up to 30 000 iterations before collecting data on parameters for 10 000 iterations. Convergence of the Markov chains was assessed visually and by the Brooks-Gelman-Rubin statistic (Brooks and Gelman 1998). We summarized the posterior distribution by the Bayesian 95% credible interval (BCI, the 2.5th and 97.5th percentile) and the median. We used the deviance information criterion (DIC) to compare models (Spiegelhalter et al. 2002). DIC is a model selection criterion

TABLE 2. Observed prevalence by age and sex class, the age–sex distribution for deer in the data, and the age–sex distribution for the modeled population based on vital rates of Wisconsin white-tailed deer.

Age (yr)	Observed prevalence		Age–sex distribution			
	Female	Male	Data		Modeled population	
			Female	Male	Female	Male
0.5	0.0034	0.0053	0.1211	0.1240	0.1881	0.1881
1.5	0.0205	0.0258	0.1165	0.1654	0.1259	0.1259
2.5	0.0424	0.0905	0.1143	0.1344	0.0842	0.0608
3.5	0.0489	0.1193	0.0739	0.0723	0.0563	0.0294
4.5–5.5	0.0643	0.1373	0.0275	0.0071	0.0629	0.0211
6.5–8.5	0.0282	0	0.0363	0.0018	0.0357	0.0057
9.5–11.5	0.0175	NA	0.0047	0	0.0107	0.0006
≥12.5	0	0	0.0006	0.0001	0.0046	0.0001

Notes: The total number of deer in the tested population was 6020 females and 6144 males. NA means that no samples of this age were obtained.

similar to the frequentist Akaike's information criteria (AIC).

We used Model 1.6 (Table 1) to test for a decline in infection probability between age class j and $j + 1$. Because of the complementary log–log form of Eq. 1, infection probability p_{ij} must decline from age j to $j + 1$ when the quantity $C_j = \beta_{j+1} - \beta_j + \log(a_{j+1}) - \log(a_j)$ is less than zero, where a_j is the tooth wear age category and β_j is the estimated effect for the age/sex class from Model 1.6. We monitored the posterior distribution of C_j for each interval between ages for each sex separately.

Prevalence standardization and map generation.—We created maps of prevalence by averaging the infection probability (p_{ij}) for a specific one-square-mile (2.59 km²) section i over the distribution of covariates (age and sex) in a standard reference population. This is known as “direct standardization” in epidemiology and has a long history (Ahmad et al. 2001). Standardized population prevalence (SPP) is calculated for the i th location as $SPP_i = \sum_j w_j p_{ij}$. Where j indexes all possible covariate classes (16 age and sex combinations, Table 2), w_j is the proportion of the standard population in covariate class j , and p_{ij} is the infection probability for class j .

To determine the proportion in each covariate class of the standard population w_j , we used the stable distribution of age and sex from a matrix model of deer demography. Specifically, w_j was calculated from the eigenvector, normalized to a sum of one, associated with the dominant real eigenvalue of the population projection matrix \mathbf{AH} (Caswell 2001). \mathbf{A} is a 26×26 matrix that defines fecundity and survival during the period of no harvest for each sex at 13 ages: fawn, yearling, adults aged 2.5–11.5 years, and adults aged ≥ 12.5 years. \mathbf{H} is a matrix whose 26 diagonal elements define the harvest survival probability and zeros elsewhere. We used high survival during the period of no harvest (0.95) and obtained fecundities from McCaffery et al. (1998) and assumed an equal sex ratio at birth. We used sex-specific harvest probabilities where antlered adult males (age ≥ 1.5 years) experience a higher harvest probability (0.48) than females and male fawns (0.28; WDNR,

unpublished data). The resulting standard population is shown in Table 2, and R code giving the details of the calculation are the Supplementary Material. We mapped the posterior median of SPP_i , and used the model with the lowest DIC to calculate infection probability p_{ij} .

RESULTS

Sample size and observed prevalence

A total of 12 164 deer were tested and had information for all covariates in our models. There were 6020 females and 6144 males in the sample. The most frequent age class was 1.5-year-old males followed by 2.5-year-old males (Table 2). The most frequent age class for females was 0.5-year-old deer with the 1.5- and 2.5-year-old deer very similar in frequency (Table 2). In contrast, the most frequent age class in the modeled distribution for both sexes was the fawn age class (0.5 years old, Table 2). The modeled population also had proportionately fewer males in the 1.5, 2.5, and 3.5 age classes than did the raw data for males. Differences between the modeled and observed age and sex structure were likely due to hunter selectivity (avoidance of fawns and preference for adult males), deliberate avoidance of testing fawns by the WDNR, sampling variance, and variation in the true population from the stable distribution that we have modeled.

Observed disease prevalence varied by age class, sex, and location (Table 2, Fig. 2). Observed prevalence was highest in the center of the study area, although some locations had very high observed prevalence outside the main cluster ($>16\%$, Fig. 2). In general, observed prevalence was low and similar between the sexes for young animals <2 years old (Table 2). Observed prevalence greatly increased for males after 2 years of age; whereas, female observed prevalence only increased moderately and appeared to decline for the older animals (Table 2).

Model selection and parameter values

The most complex polynomial model of age and sex in Set 1 was preferred by the DIC criterion (Model 1.5,

TABLE 3. The results of model fitting.

Model	pD	Deviance	DIC
Set 1			
1.1	68.7	3677.8	3746.6
1.2	68.8	3677.7	3746.5
1.3	71.0	3652.3	3723.3
1.4	70.2	3620.3	3690.5
1.5	69.0	3614.8	3683.7
1.6	77.0	3619.6	3696.6
Set 2			
2.1	72.3	3615.2	3687.5
2.2	72.9	3614.9	3687.8
2.3	78.3	3606.7	3685.0
2.4	141.5	3588.2	3729.8

Notes: Explanation of column headings: pD is a Bayesian measure of model dimensionality, and DIC (deviance information criterion) is a Bayesian model selection criterion. Smaller values of DIC indicate a better model. Boldface type indicates the model with smallest DIC within each set. Deviance is the $-2 \log(\text{likelihood})$ at the posterior mean.

Table 3). Model 1.5 was the saturated model, where each sex could have a different quadratic age-infection relationship (Table 1). The next best model in Set 1 (Model 1.4) was only slightly less complex but had a substantially higher DIC value ($\Delta\text{DIC} = 6.8$, Table 3). Therefore, this result suggests that there is substantial difference in the age-infection relationship between the sexes and the exact difference depends on the specific age (Fig. 3). In addition, location is very important for determining infection risk and the age-infection relationship (Fig. 3). Posterior distributions for specific parameters from Model 1.5 shows that the linear predictor increased with age (median $\beta_2 = 0.36$, BCI = 0.07, 0.65) and increased with the age-by-sex interaction ($\beta_3 = 0.80$, BCI = 0.27, 1.38). However, there was no significant effect for sex ($\beta_1 = -0.52$, BCI = -1.38 , 0.33). The linear predictor for Model 1.5 decreased with the square of age ($\beta_4 = -0.06$, BCI = -0.10 , -0.03) and this effect depended on sex ($\beta_5 = -0.10$, BCI = -0.20 , -0.03). The intercept ($\beta_0 = -5.14$, BCI = -5.69 , -4.60) estimates the average infection risk across all locations for females and determines the average age-infection relationship because of the multiplicative relation between the linear predictor and age (Eq. 1). Location had a large effect on infection risk (Figs. 3 and 4). The spatial random effect (α_i) varied across locations (SD = 0.76, BCI = 0.61, 0.93) and exhibited spatial dependence ($\sigma = 1.27$, BCI = 1.00, 1.60; Figs. 3 and 4), such that disease risk was mostly clustered near the center of the study area and declined toward the edges (Fig. 4).

Model 1.6, which allowed for a flexible age-prevalence relationship and an explicit test of the change in infection between age classes, did not have a lower DIC than the more complex polynomial models with age-squared terms (1.4 and 1.5, Table 3) but was much better than the simpler polynomial models without age-squared terms. Because Model 1.6 treats age as a category and Models 1.4 and 1.5 treat age as continuous,

the lower DIC suggests that there may be some change in infection risk within a season such as increasing risk for young animals and decreasing risk for older animals (Fig. 3). While the difference in DIC might be due to the relatively larger number of parameters in Model 1.6 (pD = 77.0 vs. 69.0, Table 3), it is interesting to note that the posterior mean deviance of Model 1.6 is actually larger than Model 1.5 (Table 3). Thus, Model 1.6 does not fit the data as well as the polynomial Model 1.5. The posterior probability for a decrease in infection risk between age classes from Model 1.6 was greatest for both sexes between the age classes of 4.5–5.5 and 6.5–8.5 (Table 4) just as the observed data suggested (Table 2). Posterior probabilities for other age class comparisons indicated that infection risk likely increased for younger age classes (Table 4).

In the second model set, which considered age, sex, spatial, and temporal effects on infection risk, Models 2.1 and 2.2 were nearly identical in terms of DIC and

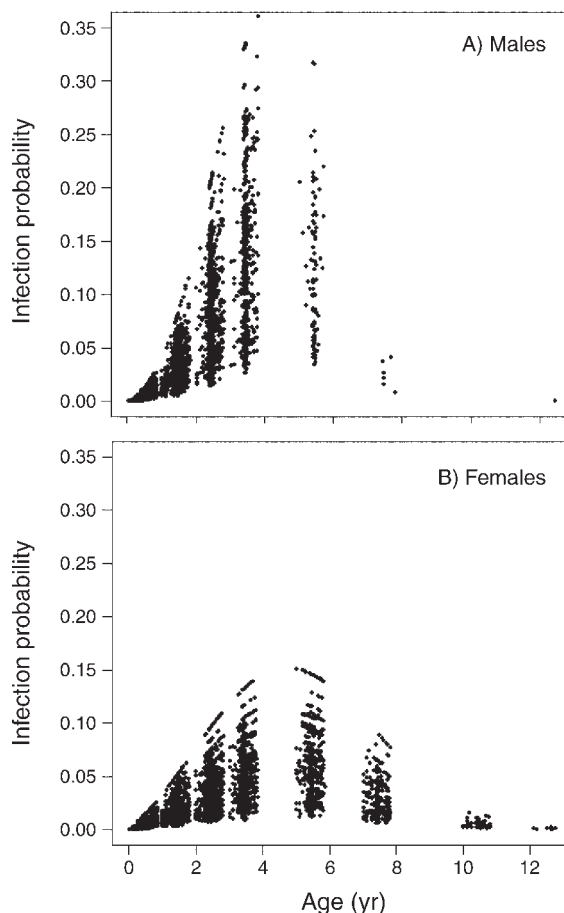


FIG. 3. The infection probability for individual deer in the data set as predicted by the covariates of age, sex, and location at the posterior median of the parameters from Model 1.5. For both (A) males and (B) females, spatial variation (the random effect α_i) across locations causes the difference in infection probability for any particular age. Ages are clustered because deer were sampled primarily during fall hunting seasons.

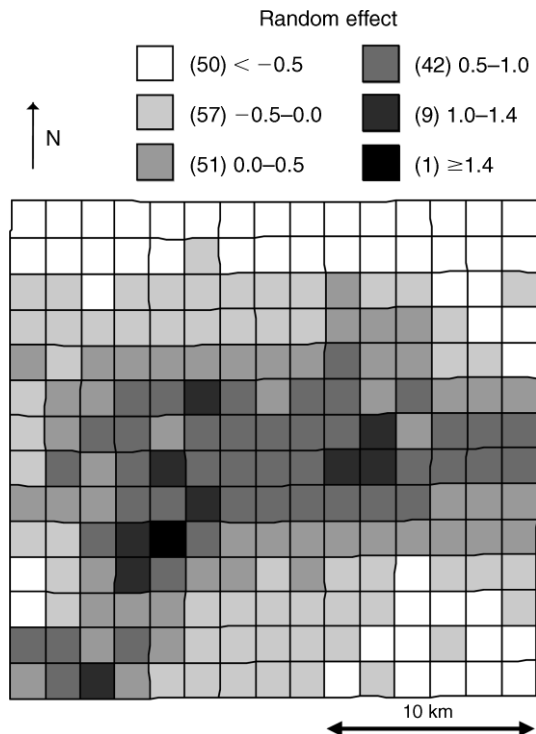


FIG. 4. Posterior median of the random effect (α_i) for Model 1.5. Each square is a section (2.59 km^2) in the modeled area (see Fig. 1). Model 1.5 only includes age and sex effects and a simple spatial random effect, which show the variation in CWD infection that is independent of age and sex variation of the sample. The number of areas in each random effect category is shown in parentheses.

only slightly worse than the best model, Model 2.3 (Table 3). Model 2.1 included a linear slope effect for year that was averaged over all areas, Model 2.2 included a random effect for each year, and Model 2.3 included both an average linear slope effect and a random slope effect that varied spatially. The most complex model of this set (Model 2.4), which allowed different spatial effects for each year, had a much larger DIC than the simpler models ($\Delta\text{DIC} > 40$, Table 3). The posterior distributions in model Set 2 for the age and sex effects were similar to those in Set 1 (results not shown),

TABLE 4. Posterior probability from Model 1.6 for a decrease in infection risk (p_{ij}) between age class j and $j + 1$.

Age class comparison		Posterior probability of decrease	
j (yr)	$j + 1$ (yr)	Female	Male
0.5	1.5	<0.001	<0.001
1.5	2.5	<0.001	<0.001
2.5	3.5	0.323	0.015
3.5	4.5–5.5	0.130	0.403
4.5–5.5	6.5–8.5	0.938	0.815
6.5–8.5	9.5–11.5	0.355	0.271
9.5–11.5	≥ 12.5	0.206	0.468

Note: The probability of an increase is the complement of a decrease.

and the posterior median for the year effect (β_6) in model 2.3 was 0.01 (BCI = $-0.06, 0.08$), indicating very little information for a consistent temporal trend. In addition, Model 2.3 was also slightly greater in DIC when compared to Model 1.5, which had no year effect ($\Delta\text{DIC} = 1.3$). Therefore, the model without any temporal trends in infection risk (Model 1.5) was an equivalent or slightly better description of the data than the model with spatiotemporal trends in infection risk (Models 2.3), again indicating that there was little evidence for an average temporal change in infection risk across locations or that individual locations were changing differently during the time span of our study.

Prevalence standardization and map generation

The posterior median of standardized population prevalence (SPP, Fig. 5) was less variable and “smoother” than that for the observed prevalence based on the sampled population (Fig. 2). SPP was also generally lower than the observed prevalence because of the larger proportion of young animals in the model-based population (Fig. 5). Prevalence at the location with the highest posterior median SPP was 0.087 (BCI = $0.063, 0.120$; Fig. 5); whereas, observed prevalence often exceeded 0.16 throughout our study area and even in areas far outside our study area (Fig. 2). When our

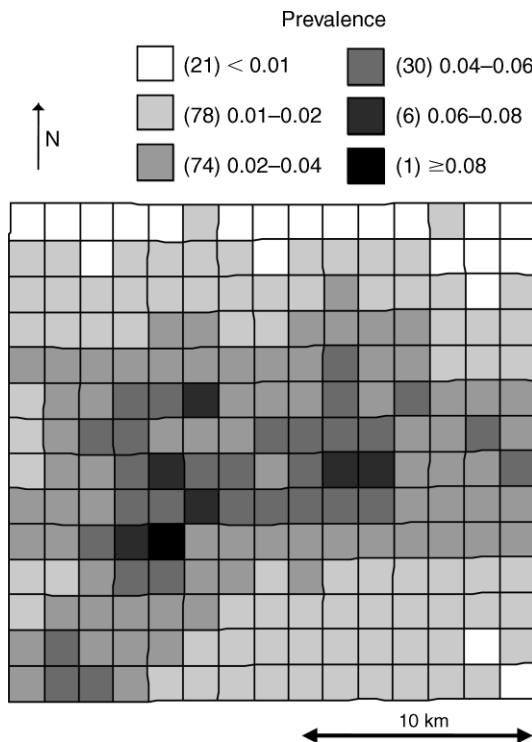


FIG. 5. Standardized population prevalence (SPP) predicted from Model 1.5 and standardized to the stable age and sex distribution from a model of deer demography (Table 2). Values shown are the median of the posterior distribution. The number of areas in each prevalence category is shown in parentheses.

model was extended to a spatial extent larger than our small area modeled here (Fig. 2, results not shown), high prevalence (>0.16) areas did not exist. Thus, much of the spatial variation in observed prevalence is due to variation of small samples and age or sex of the samples.

DISCUSSION

Understanding the distribution of disease in time and space is important for decision makers who need to apply control actions and communicate the extent and dynamics of disease to stakeholders. Unfortunately, space-time processes are among the most complicated in ecology, and data from disease systems are often complicated by host heterogeneities in infection rates due to age, sex, genotype, and the space-time epidemic process itself. In addition, sampling variation can obscure underlying disease patterns. Ignoring these complexities may lead to biased estimates of important quantities, such as prevalence. To incorporate heterogeneities in the CWD data, we used hierarchical Bayesian models to first estimate the effects of host age, sex, and location, and then we fit more complex models to estimate the temporal and space-time effects that are of interest to disease managers. We found that infection probability increased with age for young animals and increased greater for males than females. For older animals, however, infection probability declined (Fig. 3; Table 4), suggesting disease-associated mortality is affecting this population. We also found a strong influence of spatial location on infection, such that the disease was highly clustered as would be expected from an emerging infectious disease (Figs. 3 and 4). However, we found little evidence for strong temporal changes during the time span of our data. These estimates of the age and sex effects on individuals allowed us to represent spatial variation in infection risk free of the confounding effects of age and sex by standardizing disease prevalence to a constant deer population, and our standardized prevalence was lower and less variable than prevalence based on the raw data.

The age and sex patterns found in our analysis for young deer are qualitatively similar to previous analyses of CWD in Wisconsin and Colorado (Miller and Conner 2005, Grear et al. 2006, Joly et al. 2006). Based on a subset of our data, Grear et al. (2006) found that age-specific prevalence increased with age and was greater in males than females. In Colorado CWD epidemics, the age and sex patterns are similar to what we have found where males and older animals also have higher age-specific prevalence (Miller and Conner 2005). Quantitatively, however, we found that deer of intermediate ages had very high infection rates in some locations, more similar to some areas of Colorado and Wyoming (Miller and Conner 2005) than has previously been reported for Wisconsin (Grear et al. 2006, Joly et al. 2006). If there is no recovery from disease, infection should increase with age as a simple consequence of increasing cumulative infection risk (Grenfell and Anderson 1985, Heisey et al.

2006); however, the difference in infection between sexes implies sexual dimorphism in disease exposure or susceptibility as has been discussed previously (Miller and Conner 2005, Grear et al. 2006).

We found that the best model predicted a decline in age-specific prevalence after a peak near 4 to 6 years of age (Fig. 3). However, the exact appearance of this decline (Fig. 3) is likely due to the parametric nature of our models and is made more uncertain by the lack of data for old animals. Therefore, we used a more flexible model to describe the age-infection relationship (Model 1.6; Table 1), and although this model did not fit as well as the more complex polynomial models, it showed that age-specific prevalence likely declined for some older ages (Table 4). Regardless of the exact shape, age-specific prevalence will decline when the inflow of new infections does not replace those that are lost (Heisey et al. 2006). Such a decline might be caused by high force of infection with disease recovery and subsequent immunity or by declining force of infection with age combined with disease recovery or disease-associated mortality. For CWD, recovery from infection is not known to occur (Williams et al. 2002). While there is some evidence for age-related declines in susceptibility for prion diseases (Anderson et al. 1996, Heisey and Joly 2004, St Rose et al. 2006), age related changes in susceptibility alone cannot cause a decline in age-specific prevalence. Any age-related decline in susceptibility or exposure alone would only cause age-specific prevalence to asymptote (Heisey et al. 2006), but in combination with disease-associated mortality a decline in susceptibility or exposure will cause the decline in age-specific prevalence. Therefore, the most parsimonious explanation for any decline in prevalence for older animals is disease-associated mortality in combination with an age-related decline in force of infection. Of course, sampling or observation biases in our hunter-collected data might contribute to the observed age-infection relationship (Conner et al. 2000, Jennelle et al. 2007). For example, hunters may be more likely to shoot infected deer. For this type of bias to significantly affect the observed patterns, young positive animals (near the age of peak infection, Fig. 3) would need to experience higher hunting mortality. While this interaction between age and harvest bias is possible, it is complex and, if present, the bias itself is a form of disease-associated mortality: increased mortality of young infected animals due to increased hunter vulnerability.

Despite fitting the more complex models of the space-time dynamics (model Set 2; Table 2), we could not find any strong evidence for a consistent temporal trend or location-specific temporal trends that might be expected during an epidemic. Our models without a temporal trend had a smaller (but nearly identical) DIC than models with temporal trends (Model 1.5 compared to Model 2.3). In addition, the posterior estimate of the yearly rate of change in Model 2.3 greatly overlapped zero. Clearly, there is very little information regarding a

change in prevalence from these data and models. In contrast, CWD prevalence for mule deer in Colorado was found to more than double in some populations over 7 years (Miller and Conner 2005). Our results, however, do not mean that CWD is not spreading across the landscape or not changing in prevalence within our study area. In fact, the clumped disease distribution itself (Figs. 2 and 3) suggests that CWD has spread in the past just as an emerging infectious disease is expected to behave, and our posterior distribution for temporal parameters indicate that CWD may have increased or decreased relatively rapidly during the 5 years of data (posterior probability for an increase ~ 0.50). Additionally, long-distance dispersal of the disease may be spreading CWD at relatively low prevalence across a larger spatial extent than we have modeled. If this is the case, then CWD could spread spatially in a largely unpredictable and undetectable manner than is evident from our results (Clark et al. 2003). When more data are available across a larger range of years, perhaps the spatiotemporal models used here will have stronger support for estimating the dynamics of CWD in Wisconsin.

We are left with the conclusion that measurement of spatially explicit temporal change in CWD is unlikely over moderate time periods and spatial scales, despite the relatively sophisticated methods and large sample size used here. Conner et al. (2007) also examined CWD prevalence trends in Colorado populations of mule deer that were culled with variable intensity and could not find any evidence for a change in prevalence over short time periods (2–4 years) due to culling. Because they were in essence trying to detect spatial variation in the rate of prevalence change, their result is consistent with our result that models with spatially heterogeneous rates of change were no better than simpler models (Table 3). Therefore, time series much greater than 5 years or much larger manipulations of management actions or environmental conditions will be needed to reliably detect spatial heterogeneity in CWD dynamics. Alternatively, this CWD epidemic may grow at a faster rate in the future, as might be expected as infectious prion accumulates in the environment, and then detection of spatiotemporal trends might be more likely.

Finally, we used the best model (Model 1.5) and the stable age distribution from a model of host demography to standardized prevalence across our study area (Fig. 5). We did this because prevalence must be standardized to a constant population distribution of important covariates when comparing across regions (Ahmad et al. 2001), and standardized prevalence is more directly meaningful to managers and decision-makers than is a single age-specific prevalence or the spatial random effect, which in our models represents the relative difference in prevalence across space but on the complimentary log-log scale. Standardized prevalence has the advantage that it represents the likelihood that a randomly selected animal from a specific

population and area is positive, and this is biologically meaningful for informed disease management or regulation development. For example, standardized prevalence can be used to draw management boundaries, design surveillance programs, and predict the resources needed to detect or remove positive animals from the landscape. By basing these decisions on a specific age and sex distribution, the assumptions behind the calculation are clear or can be easily changed if a different population is of interest.

While the stable age distribution that we have used may not reflect the actual distribution of age and sex in our study area, the choice of a standard is arbitrary for representing the variation in disease across space (Ahmad et al. 2001). We believe, however, that the stable age distribution is a reasonable choice when unbiased data are lacking, such as in our case where some fawns were intentionally not tested and where we suspect hunters are not randomly sampling deer (Roseberry and Klimstra 1974, Kubisiak et al. 2001).

CWD is an emerging infectious disease being found in new locations within Wisconsin and across North America each year. Very little is currently known about the consequences of this disease to wildlife, livestock, or human health, but management agencies are increasingly confronted with the presence of CWD. A first step to any management decision is an estimate of the disease distribution and how this distribution is changing. Because of the complex space-time process of emerging disease, heterogeneities in the host population, and sampling variation, understanding the patterns of CWD necessitates the use of statistical models that can incorporate these effects. Fortunately, these methods are widely available and easily implemented because of work in human disease mapping (Lawson et al. 2003, Spiegelhalter et al. 2004), and ecologists working on wildlife disease should incorporate use of these techniques when examining spatial and temporal patterns.

ACKNOWLEDGMENTS

This paper could not be possible without the hard work from many volunteers and staff in the WDNR. Comments from Matt Farnsworth, Tim Linksvayer, Dan Storm, Stacie Robinson, Delwyn Keane, and two anonymous reviewers improved this work. Funding was provided by the WDNR and the Wisconsin Cooperative Wildlife Research Unit. Mention of trade names or commercial products does not imply endorsement by the U.S. Government.

LITERATURE CITED

- Ahmad, O. B., C. Boschi-Pinto, A. D. Lopez, C. J. L. Murray, R. Lozano, and M. Inoue. 2001. Age standardization of rates: a new WHO standard. GPE Discussion Paper Series No. 31, World Health Organization, Geneva, Switzerland.
- Anderson, R. M., et al. 1996. Transmission dynamics and epidemiology of BSE in British cattle. *Nature* 382:779–788.
- Bernardinelli, L., D. Clayton, C. Pascutto, C. Montomoli, M. Ghislandi, and M. Songini. 1995. Bayesian analysis of space-time variation in disease risk. *Statistics in Medicine* 14:2433–2443.
- Besag, J., J. York, and A. Mollie. 1991. Bayesian image restoration with two applications in spatial statistics. *Annals of the Institute of Statistical Mathematics* 43:1–59.

- Best, N., S. Richardson, and A. Thomson. 2005. A comparison of Bayesian spatial models for disease mapping. *Statistical Methods in Medical Research* 14:35–59.
- Blanchong, J. A., D. O. Joly, M. D. Samuel, J. A. Langenberg, R. E. Rolley, and J. F. Sausen. 2006. White-tailed deer harvest from the chronic wasting disease eradication zone in south-central Wisconsin. *Wildlife Society Bulletin* 34:725–731.
- Brooks, S. P., and A. Gelman. 1998. General methods for monitoring convergence of iterative simulations. *Journal of Computational and Graphical Statistics* 7:434–455.
- Caley, P., and J. Hone. 2002. Estimating the force of infection; *Mycobacterium bovis* infection in feral ferrets *Mustela furo* in New Zealand. *Journal of Animal Ecology* 71:44–54.
- Caswell, H. 2001. *Matrix population models: construction, analysis, and interpretation*. Second edition. Sinauer Associates, Sunderland, Massachusetts, USA.
- Clark, J. S. 2005. Why environmental scientists are becoming Bayesians. *Ecology Letters* 8:2–14.
- Clark, J. S., and A. E. Gelfand. 2006. A future for models and data in environmental science. *Trends in Ecology and Evolution* 21:375–380.
- Clark, J. S., M. Lewis, J. S. McLachlan, and J. HilleRisLambers. 2003. Estimating population spread: what can we forecast and how well? *Ecology* 84:1979–1988.
- Conner, M. M., C. W. McCarty, and M. W. Miller. 2000. Detection of bias in harvest-based estimates of chronic wasting disease prevalence in mule deer. *Journal of Wildlife Diseases* 36:691–699.
- Conner, M. M., M. W. Miller, M. R. Ebinger, and K. P. Burnham. 2007. A meta-BACI approach for evaluating management intervention on chronic wasting disease in mule deer. *Ecological Applications* 17:140–153.
- Elliott, P., J. C. Wakefield, N. Best, and D. J. Briggs. 2000. *Spatial epidemiology: methods and applications*. Oxford University Press, Oxford, UK.
- Ellison, A. M. 2004. Bayesian inference in ecology. *Ecology Letters* 7:509–520.
- Farnsworth, M. L., J. A. Hoeting, N. T. Hobbs, and M. W. Miller. 2006. Linking chronic wasting disease to mule deer movement scales: a hierarchical Bayesian approach. *Ecological Applications* 16:1026–1036.
- Gelman, A., J. B. Carlin, H. S. Stern, and D. B. Rubin. 2004. *Bayesian data analysis*. Second edition. Chapman and Hall, New York, New York, USA.
- Grear, D. A., M. D. Samuel, J. A. Langenberg, and D. Keane. 2006. Demographic patterns and harvest vulnerability of chronic wasting disease infected white-tailed deer in Wisconsin. *Journal of Wildlife Management* 70:546–553.
- Grenfell, B. T., and R. M. Anderson. 1985. The estimation of age-related rates of infection from case notifications and serological data. *Journal of Hygiene, Cambridge* 95:419–436.
- Hastings, A., et al. 2005. The spatial spread of invasions: new developments in theory and evidence. *Ecology Letters* 8:91–101.
- Heisey, D. M., and D. O. Joly. 2004. Age and transmissible spongiform encephalopathies. *Emerging Infectious Diseases* 10:1164–1165.
- Heisey, D. M., D. O. Joly, and F. Messier. 2006. The fitting of general force-of-infection models to wildlife disease prevalence data. *Ecology* 87:2356–2365.
- Hosseini, P. R., A. A. Dhondt, and A. P. Dobson. 2006. Spatial spread of an emerging infectious disease: conjunctivitis in house finches. *Ecology* 87:3037–3046.
- Jennelle, C. S., E. G. Cooch, M. J. Conroy, and J. C. Senar. 2007. State-specific detection probabilities and disease prevalence. *Ecological Applications* 17:154–167.
- Johnson, C. J., J. A. Pedersen, R. J. Chappell, D. McKenzie, and J. M. Aiken. 2007. Oral transmissibility of prion disease is enhanced by binding to soil particles. *PLoS Pathogens* 3:e93.
- Johnson, C. J., K. E. Phillips, P. T. Schramm, D. McKenzie, J. M. Aiken, and J. A. Pedersen. 2006. Prions adhere to soil minerals and remain infectious. *PLoS Pathogens* 2:296–302.
- Joly, D. O., C. A. Ribic, J. A. Langenberg, K. Beheler, C. A. Batha, B. J. Dhuey, R. E. Rolley, G. Bartelt, T. R. Van Deelen, and M. D. Samuel. 2003. Chronic wasting disease in free-ranging Wisconsin white-tailed deer. *Emerging Infectious Diseases* 9:599–601.
- Joly, D. O., M. D. Samuel, J. A. Langenberg, J. A. Blanchong, C. A. Batha, R. E. Rolley, D. P. Keane, and C. A. Ribic. 2006. Spatial epidemiology of chronic wasting disease in Wisconsin white-tailed deer. *Journal of Wildlife Diseases* 42:578–588.
- Keane, D. P., D. J. Barr, J. E. Keller, S. M. Hall, J. A. Langenberg, and P. N. Bochler. 2008. Comparison of retropharyngeal lymph node and obex region of the brainstem in detection of chronic wasting disease in white-tailed deer (*Odocoileus virginianus*). *Journal of Veterinary Diagnostic Investigation* 20:58–60.
- Keeling, M. J. 1999. The effects of local spatial structure on epidemiological invasions. *Proceedings of the Royal Society B* 266:859–867.
- Kubisiak, J. F., K. R. McCaffery, W. A. Creed, T. A. Heberlein, R. C. Bishop, and R. E. Rolley. 2001. Sandhill whitetails: providing new perspectives for deer management. Wisconsin Department of Natural Resources, Madison, Wisconsin, USA.
- LaDeau, S. L., A. M. Kilpatrick, and P. P. Marra. 2007. West Nile virus emergence and large-scale declines of North American bird populations. *Nature* 447:710–U713.
- Lawson, A. B. 2006. *Statistical methods in spatial epidemiology*. Second edition. John Wiley and Sons, West Sussex, UK.
- Lawson, A. B., W. J. Browne, and C. L. Vidal Rodeiro. 2003. *Disease mapping with WinBUGS and MLwiN*. John Wiley and Sons, Chichester, UK.
- Lichstein, J. W., T. R. Simons, S. A. Shriener, and K. E. Franzreb. 2002. Spatial autocorrelation and autoregressive models in ecology. *Ecological Monographs* 72:445–463.
- Lunn, D., A. Thomas, N. Best, and D. J. Spiegelhalter. 2000. WinBUGS—a Bayesian modelling framework: concepts, structure, and extensibility. *Statistics and Computing* 10:325–337.
- Mathiasen, C. K., et al. 2006. Infectious prions in the saliva and blood of deer with chronic wasting disease. *Science* 314:133–136.
- McCaffery, K. R., J. E. Ashbrenner, and R. E. Rolley. 1998. Deer reproduction in Wisconsin. *Transactions of the Wisconsin Academy of Sciences, Arts, and Letters* 86:249–261.
- Miller, M. W., and M. M. Conner. 2005. Epidemiology of chronic wasting disease in free-ranging mule deer: spatial, temporal, and demographic influences on observed prevalence patterns. *Journal of Wildlife Diseases* 41:275–290.
- Miller, M. W., N. T. Hobbs, and S. J. Taverer. 2006. Dynamics of prion disease transmission in mule deer. *Ecological Applications* 16:2208–2214.
- Miller, M. W., and E. S. Williams. 2003. Horizontal prion transmission in mule deer. *Nature* 425:35–36.
- Miller, M. W., E. S. Williams, N. T. Hobbs, and L. L. Wolfe. 2004. Environmental sources of prion transmission in mule deer. *Emerging Infectious Diseases* 10:1003–1006.
- Moore, D. A. 1999. Spatial diffusion of raccoon rabies in Pennsylvania, USA. *Preventive Veterinary Medicine* 40:19–32.
- Ostfeld, R. S., G. E. Glass, and F. Keesing. 2005. Spatial epidemiology: an emerging (or re-emerging) discipline. *Trends in Ecology and Evolution* 20:328–336.
- Richardson, S., A. Thomson, N. Best, and P. Elliott. 2004. Interpreting posterior relative risk estimates in disease-mapping studies. *Environmental Health Perspectives* 112:1016–1025.

- Roseberry, J. L., and W. D. Klimstra. 1974. Differential vulnerability during a controlled deer harvest. *Journal of Wildlife Management* 38:499–507.
- Samuel, M. D., D. O. Joly, M. A. Wild, S. D. Wright, D. L. Otis, R. W. Werge, and M. W. Miller. 2003. Surveillance strategies for detecting chronic wasting disease in free-ranging deer and elk. U.S. Geological Survey, National Wildlife Health Center, Madison, Wisconsin, USA.
- Severinghaus, C. W. 1949. Tooth development and wear as criteria of age in white-tailed deer. *Journal of Wildlife Management* 13:195–216.
- Smith, D. L., B. Lucey, L. A. Waller, J. E. Childs, and L. A. Real. 2002. Predicting the spatial dynamics of rabies epidemics on heterogeneous landscapes. *Proceedings of the National Academy of Sciences (USA)* 99:3668–3672.
- Spiegelhalter, D. J., N. G. Best, B. R. Carlin, and A. van der Linde. 2002. Bayesian measures of model complexity and fit. *Journal of the Royal Statistical Society Series B* 64:583–616.
- Spiegelhalter, D. J., A. Thomas, N. G. Best, and D. Lunn. 2004. WinBugs user manual. Version 1.4.1. MRC Biostatistics Unit, Cambridge, UK.
- St Rose, S. G., N. Hunter, L. Matthews, J. D. Foster, M. E. Chase-Topping, L. E. B. Kruuk, D. J. Shaw, S. M. Rhind, R. G. Will, and M. E. J. Woolhouse. 2006. Comparative evidence for a link between Peyer's patch development and susceptibility to transmissible spongiform encephalopathies. *BMC Infectious Diseases* 6.
- Szklo, M., and F. J. Nieto. 2007. *Epidemiology: beyond the basics*. Second edition. Jones and Bartlett Publishers, Boston, Massachusetts, USA.
- Wakefield, J. C., N. G. Best, and L. Waller. 2000. Bayesian approaches to disease mapping. Pages 104–127 in P. Elliott, J. C. Wakefield, N. G. Best, and D. J. Briggs, editors. *Spatial epidemiology: methods and applications*. Oxford University Press, Oxford, UK.
- Waller, L. A. 1997. Hierarchical spatiotemporal mapping of disease rates. *Journal of the American Statistical Association* 92:607–617.
- Waller, L. A., B. P. Carlin, H. Xia, and A. E. Gelfand. 1997. Hierarchical spatio-temporal mapping of disease rates. *Journal of the American Statistical Association* 92:607–617.
- Wikle, C. K. 2003. Hierarchical Bayesian models for predicting the spread of ecological processes. *Ecology* 84:1382–1394.
- Williams, E. S., and M. W. Miller. 2003. Transmissible spongiform encephalopathies in non-domestic animals: origin, transmission and risk factors. *Revue Scientifique et Technique de l'Office International des Epizooties* 22:145–156.
- Williams, E. S., M. W. Miller, T. J. Kreeger, R. H. Kahn, and E. T. Thorne. 2002. Chronic wasting disease of deer and elk: a review with recommendations for management. *Journal of Wildlife Management* 66:551–563.

SUPPLEMENT

Source code for WinBUGS and R programs described in the text (*Ecological Archives* A019-052-S1).